CHEMISTRY OF MATERIALS
Article

Chem. Mater. **2010,** *22,* 5973–5982 5973
DOI:10.1021/cm102156v

Insights into Reversible Dissolution of Colloidal CdSe Nanocrystal Quantum Dots

Jacqueline T. Siy and Michael H. Bartl*

Department of Chemistry, University of Utah, 315 South 1400 East, Salt Lake City, Utah 84112, United States

Received July 31, 2010. Revised Manuscript Received September 21, 2010

The dissolution behavior of colloidal CdSe nanocrystal quantum dots is investigated. A series of experiments is conducted to study the stability of nanocrystals based on a simple reversible dissolution-growth reaction model. Immersing purified CdSe quantum dots in a fresh solvent at elevated temperatures resulted in their dissolution with rates determined by their concentration, size, type and amount of ligands present in solution, and temperature. In general, highest dissolution rates were observed for diluted quantum dot solutions in the presence of phosphonic acids and carboxylic acids ligands, at temperatures below 200 °C. Importantly, the dissolution process is reversible and regrowth of quantum dots occurs at temperatures above 220 °C. It is concluded that the most stable state of nanocrystal quantum dots in solution is an equilibrium between formed crystals and free molecular precursors in solution.

Introduction

Semiconductor nanocrystals possess a size-dependent discrete energy level distribution, lending them tunable electronic and optical properties with well-defined optical absorption features and narrow luminescence emission bands with high quantum yields.[1−3] These properties make nanocrystals promising candidates for emerging applications ranging from biological labeling and imaging[4,5] to light-emitting diodes,[6] microlasing,[7−9] and solar energy conversion.[10−12] This wide array of potential applications has sparked research into developing robust and simple synthesis routes for the fabrication of high-quality colloidal nanocrystals. In 1993 Murray, Norris, and Bawendi reported a "hot injection" synthesis method for nearly monodisperse colloidal cadmium chalcogenide nanocrystal quantum dots (QDs) based on colloidal crystal nucleation and growth chemistry of organometallic cadmium and chalcogenide precursors in the presence of a long alkyl-chain ligand/solvent system.[13] Following this seminal work, widespread research efforts have been focused on studying the formation mechanism of nanocrystals.[14−21] These studies have not only resulted in new insights into the nanocrystal formation mechanism, but have also led to a generalization of this colloidal synthesis approach. To date, a large variety of colloidal nanocrystal formation procedures using inexpensive, readily available and "green" reaction components is available, resulting in an enormous range of nanocrystals with different compositions, sizes, and shapes, including dots, rods, tetrapods, and multicompositional semiconductor heterostructures.[22−30]

*Corresponding author. E-mail: bartl@chem.utah.edu.

(1) Alivisatos, A. P. *Science* **1996**, *271*, 933–937.
(2) Brus, L. E. *J. Phys. Chem.* **1986**, *90*, 2555–2560.
(3) Burda, C.; Chen, X.; Narayanan, R.; El-Sayed, M. A. *Chem. Rev.* **2005**, *105*, 1025–1102.
(4) Bruchez, M., Jr.; Moronne, M.; Gin, P.; Weiss, S.; Alivisatos, A. P. *Science* **1998**, *281*, 2013–2016.
(5) Walkey, C.; Sykes, E. A.; Chan, W. C. W. *Hematology* **2009**, *2009*, 701–707.
(6) Tessler, N.; Medvedev, V.; Kazes, M.; Kan, S.; Banin, U. *Science* **2002**, *295*, 1506.
(7) Cha, J. N.; Bartl, M. H.; Wong, M. S.; Popitsch, A.; Deming, T. J.; Stucky, G. D. *Nano Lett.* **2003**, *3*, 907–911.
(8) Klimov, V. I.; Ivanoc, S. A.; Nanda, J.; Achermann, M.; Bezel, I.; McGuire, J. A.; Piryatinski, A. *Nature* **2007**, *447*, 441–446.
(9) Kazes, M.; Lewis, D. Y.; Ebenstein, Y.; Mokari, T.; Banin, U. *Adv. Mater.* **2002**, *14*, 317–321.
(10) Gur, I.; Fromer, N. A.; Geier, M. L.; Alivisatos, A. P. *Science* **2005**, *310*, 462.
(11) Kumar, S.; Scholes, G. D. *Microchim. Acta* **2008**, *160*, 315–325.
(12) Milliron, D. J.; Gur, I.; Alivisatos, A. P. *MRS Bull.* **2005**, *30*, 41.
(13) Murray, C. B.; Norris, D. J.; Bawendi, M. G. *J. Am. Chem. Soc.* **1993**, *115*, 8706–8715.
(14) Bullen, C. R.; Mulvaney, P. *Nano Lett.* **2004**, *4*, 2303–2307.
(15) Xie, R.; Li, Z.; Peng, X. *J. Am. Chem. Soc.* **2009**, *131*, 15457–15466.
(16) Peng, X. *Nano Research* **2009**, *2*, 425–447.
(17) Chuang, X.; Hongxun, H.; Wei, C.; Jingkang, W. *J. Cryst. Growth* **2008**, *310*, 3504–3507.
(18) Park, J.; Lee, K. H.; Galloway, J. F.; Searson, P. C. *J. Phys. Chem. C* **2008**, *112*, 17849–17854.
(19) Qu, L.; Yu, W. W.; Peng, X. *Nano Lett.* **2004**, *4*, 465–469.
(20) Yu, K.; Hu, M. Z.; Wang, R.; Piolet, M. l. L.; Frotey, M.; Zaman, M. B.; Wu, X.; Leek, D. M.; Tao, Y.; Wilkinson, D.; Li, C. *J. Phys. Chem. C* **2010**, *114*, 3329–3339.
(21) Liu, H.; Owen, J. S.; Alivisatos, A. P. *J. Am. Chem. Soc.* **2006**, *129*, 305–312.
(22) Liu, X.; Lin, Y.; Chen, Y.; An, L.; Ji, X.; Jiang, B. *Chem. Lett.* **2005**, *34*, 1284–1285.
(23) Cumberland, S. L.; Hanif, K. M.; Javier, A.; Khitrov, G. A.; Strouse, G. F.; Woessner, S. M.; Yun, C. S. *Chem. Mater.* **2002**, *14*, 1576–1584.
(24) Deng, Z.; Cao, L.; Tang, F.; Zou, B. *J. Phys. Chem. B* **2005**, *109*, 16671–16675.
(25) Caruso, F., ed. *Colloids and Colloid Assemblies*; Wiley-VCH: Weinheim, 2003.
(26) Efros, A. L.; Lockwood, D. J.; Tsybeskov, L., *Semiconductor Nanocrystals: From Basic Principles to Applications*; Springer: New York, 2003.
(27) Shen, H.; Wang, H.; Chen, X.; Niu, J. Z.; Xu, W.; Li, X. M.; Jiang, X.-D.; Du, Z.; Li, L. S. *Chem. Mater.* **2010**, *22*, 4756−4761.

Published on Web 10/13/2010

Of equal importance to studies on how nanocrystals are formed is the knowledge about the "reverse" reaction: the dissolution of nanocrystals. The significance of the dissolution process of nanocrystals is 2-fold: First, dissolution strongly affects the postsynthesis stability of nanocrystals and therefore is of great importance for their long-term use in all solution-based applications. This is especially the case for use of nanocrystals as optical labels in biological imaging. Here, dissolution can have severe implications due to the long metabolic lifetime and high toxicity of widely used nanocrystal components such as cadmium or lead.[31] Second, understanding dissolution behavior is of great importance for the rational design of efficient synthesis routes for high-quality nanocrystals. Since dissolution is the competing reaction to nanocrystal formation, a detailed knowledge of parameters that favor dissolution is essential for successful growth reactions.

Despite the importance of nanocrystal dissolution for both the successful nanocrystal formation and their safe and prolonged use in most applications, very little is known about its underlying mechanism and reaction pathways. Most of the present knowledge about nanocrystal dissolution is the result of incidental observations during ligand-exchange reactions or is deduced from experimental and theoretical studies concerned mostly with nanocrystal formation.[32−39] While the main focus of these works is on developing general models describing the nucleation and growth mechanism of nanocrystal synthesis, they also provide valuable insights into experimental parameters that can influence the equilibrium between growth and dissolution of nanocrystals in solution.

An important study in this regard has been conducted by Alivisatos and co-workers.[21] By investigating the evolution of the molecular organometallic precursors during the formation/growth of II−VI nanocrystal QDs, they were able to provide new insights regarding how the surface ligands controlled the growth dynamics of the nanocrystals. In detail, they found that the concentration of ligands in the synthesis solution greatly influences the solubility of the molecular precursor compounds, as well as the degree of their conversion into high-quality semiconductor nanocrystal QDs. Moreover, their study revealed that the nanocrystals cease to grow while there is still a substantial amount of molecular precursor free in solution. These findings thus suggest that the most stable thermodynamic state of nanocrystals is a coexistence of the formed nanocrystals and free molecular precursor species in solution—a balance between growth and dissolution.

In this paper, we present a series of experiments designed to investigate the relationship between growth and dissolution of colloidal nanocrystal QDs by systematically studying the dissolution/growth behavior of beforehand-synthesized nanocrystal QDs in solution. Particular focus will be on dissolution as a function of QD size and concentration, the type of ligands (carboxylic acid and amine based) present in the solution, the relative ratio of ligand concentration to QD surface area, and reaction temperature. Our model system consists of purified, surface ligand-stabilized colloidal CdSe nanocrystal QDs in a noncoordinating solvent (with or without excess ligands) and under inert-gas atmosphere at a temperature of at least 100 °C. The dissolution/growth events are monitored by UV−vis absorption spectroscopy, photoluminescence studies and electron microscopy imaging. For example, we found that immersing purified CdSe nanocrystal QDs in a fresh solvent at elevated temperatures can induce a dissolution event. While dissolution of CdSe nanocrystal QDs in pure solvent is slow, the rate of this process is significantly enhanced in the presence of excess ligands. However, we also observed that the dissolution process can be reversed at any time by changing the reaction parameters (e.g., relative concentrations of nanocrystals and molecular precursors and the reaction temperature), resulting in nanocrystal regrowth. Our results thus point to a delicate interplay between nanocrystal dissolution and growth with the most stable state being coexistence between free molecular monomers and nanocrystals in solution. We compare our results to growth studies and deduce nanocrystal-size-dependent stability parameters.

Experimental Section

Materials. All chemical reagents and solvents used were purchased from commercial suppliers and were used without further purification. Cadmium acetate dihydrate (Aldrich, 98%), cadmium oxide (Aldrich, 99.99+%), octadecylamine and octylamine (ODA and OcA, respectively, Aldrich, 97%), 1-octadecene (ODE, Aldrich, 90%), selenium (Aldrich, 99.99%), stearic acid (SA, Alfa Aesar, 99%), oleic acid (OA, Aldrich, 97%), trioctylphosphine (TOP, Aldrich, 90%), and trioctylphosphine oxide (TOPO, Aldrich, 99) All moisture/air sensitive chemicals were stored under nitrogen atmosphere.

Synthesis of CdSe Nanocrystal Quantum Dots. All nanocrystal size-reduction experiments were conducted on purified CdSe nanocrystal QDs synthesized by a modified hot injection method adapted from Peng and co-workers.[40] All reactions were done under argon atmosphere. Briefly, 0.08 g of cadmium acetate dihydrate was dissolved in 3.0 g stearic acid (SA) in a three-neck

(28) Viswanatha, R.; Battaglia, D.; Curtis, M.; Mishima, T.; Johnson, M.; Peng, X. *Nano Res.* **2008**, *1*, 138–144.
(29) Manna, L.; Scher, E. C.; Alivisatos, A. P. *J. Am. Chem. Soc.* **2000**, *122*, 12700–12706.
(30) Oluwafemi, O. S.; Revaprasadu, N. *New. J. Chem.* **2008**, *10*, 1432–1437.
(31) Fitzpatrick, J. A. J.; Andreko, S. K.; Ernst, L. A.; Waggoner, A. S.; Ballou, B.; Bruchez, M. P. *Nano Lett.* **2009**, *9*, 2736–2741.
(32) Li, R.; Luo, Z.; Papadimitrakopoulos, F. *J. Am. Chem. Soc.* **2006**, *128*, 6280–6281.
(33) Talapin, D. V.; Rogach, A. L.; Kornowski, A.; Haase, M.; Weller, H. *Nano Lett.* **2001**, *1*, 207–211.
(34) Dai, Q.; Li, D.; Chen, H.; Kan, S.; Li, H.; Gao, S.; Hou, Y.; Liu, B.; Zou, G. *J. Phys. Chem. B* **2006**, *110*, 16508–16513.
(35) Landes, C.; Braun, M.; Burda, C.; El-Sayed, M. A. *Nano Lett.* **2001**, *1*, 667–670.
(36) Li, R.; Lee, J.; Kang, D.; Luo, Z.; Aindow, M.; Papadimitrakopoulos, F. *Adv. Funct. Mater.* **2006**, *16*, 345–350.
(37) Li, R.; Lee, J.; Yang, B.; Horspool, D. N.; Aindow, M.; Papadimitrakopoulos, F. *J. Am. Chem. Soc.* **2005**, *127*, 2524–2532.
(38) Munro, A. M.; Jen-La Plante, I.; Ng, M. S.; Ginger, D. S. *J. Phys. Chem. C* **2007**, *111*, 6220–6227.
(39) Rempel, J. Y.; Bawendi, M. G.; Jensen, K. F. *J. Am. Chem. Soc.* **2009**, *131*, 4479–4489.
(40) Qu, L.; Peng, Z. A.; Peng, X. *Nano Lett.* **2001**, *1*, 333–337.

round-bottom flask. This solution was heated to 130 °C using an oil bath until a clear solution was obtained. After the solution was allowed to cool to room temperature and aged overnight, 3.0 g trioctylphosphine oxide (TOPO) was added. The selenium precursor was prepared in a separate flask by mixing 0.085 g elemental selenium with 4.5 mL trioctylphosphine (TOP) and 0.4 mL toluene at room temperature. The cadmium-precursor flask was heated to 340 °C using a heating mantle, and 3.5 mL TOPSe was injected into it. After a certain time, the reaction was stopped by cooling the reaction temperature to 60−80 °C. The purification process consisted of precipitation/redissolution with acetone/hexanes, followed by ethanol/hexanes. QD size and concentration were calculated from the wavelength position of the first excitonic absorption transition.[41] Highly monodisperse CdSe nanocrystal QDs with sizes ranging from 3.0 to 6.0 nm, depending on the growth conditions, were obtained by this method.

Dissolution Studies of CdSe Nanocrystal Quantum Dots. For the dissolution experiments, purified CdSe nanocrystal QDs were immersed in a noncoordinating organic solvent such as octadecene (ODE) in the presence of fresh surface-stabilizing ligands such as SA, oleic acid (OA), or octadecylamine (ODA), followed by heating to elevated temperatures under an inert gas atmosphere (argon gas). In a typical experiment 1 mL of a hexanes solution of CdSe QDs with a concentration of 10^{-6} M were filled into a three-neck round-bottom flask together with 0.5 g ODA and 5−20 mL ODE. This mixture was first stirred at room temperature under vacuum for 30 min to remove dissolved gases and then heated to 100 °C. After maintaining the mixture at 100 °C for about 10 min (to completely remove hexanes from the reaction mixture) the atmosphere was switched from vacuum to argon. Samples were then either maintained at 100 °C or heated to higher temperatures. To monitor the reaction, aliquots were taken at given time intervals for optical spectroscopy and electron microscopy investigations. Reactions were stopped by cooling the solutions to temperatures below 50 °C. The nanocrystal samples are then purified by first diluting the reaction mixtures with hexanes (1:1 by volume) followed by adding methanol (twice the amount of hexanes used) and vigorous mixing. The hexane layer was extracted and the nanocrystals were precipitated with acetone. For experiments where OA and SA were used, nanocrystal purification was achieved by addition of hexanes (1:1 by volume) and direct precipitation with ethanol (twice the amount of hexanes added). All precipitated nanocrystal samples were further washed with acetone, redissolved in hexanes, and stored under nitrogen atmosphere.

Optical Measurements. UV−vis absorption spectra were measured on an Ocean Optics USB2000 fiber optic spectrometer. Photoluminescence (PL) spectra were recorded on a Fluorolog FL3-22 fluorescence spectrometer with the excitation wavelength set at 450 nm. PL images were taken under UV illumination at 360 nm using a mercury lamp.

Transmission Electron Microscopy (TEM). TEM images were taken using a FEI Tecnai F30 transmission electron microscope operating at an acceleration voltage of 300 kV. The purified nanocrystals dissolved in hexanes were deposited onto Carbon Type B TEM sample holder grids from Ted Pella.

Powder X-ray Diffraction (XRD). Diffraction patterns were obtained from powdered samples of CdSe nanocrystals with a Bruker D8 Advanced X-ray Diffractometer.

Cross-polarization Magic-angle Spinning Nuclear Magnetic Resonance (CP MAS NMR). ^{13}C-^{1}H CP MAS NMR and ^{31}P-^{1}H CP MAS NMR experiments were conducted on CdSe samples using an Infinity Plus 600 Varian solid-state NMR instrument.

Size Determination of Nanocrystals. Direct size determination of QDs was done by TEM imaging. The diameter of at least 25 nanocrystals was measured from TEM images and the average size and standard deviation was determined. The diameter standard deviations were determined to be 0.5 nm. To accurately determine the relative (small) size changes of the nanocrystal QDs during the dissolution events, we used the method derived by Peng and co-workers.[41] This method allows size determination by comparing the wavelength position of the first excitonic absorption peak maxima of differently sized CdSe QDs. The corresponding uncertainty of the QD sizes were determined by evaluating the uncertainty in the wavelength position of the first excitonic absorption peak (±1 nm) and the general error propagation formula applied to sizing equation of ref 41. The QD size evolution uncertainties were calculated to be 0.05 to 0.1 nm in diameter. For all dissolution experiments this absorption spectroscopy-based size-determination method was used to evaluate the relative changes in QD size.

Results and Discussion

The Dissolution-Growth Model System. The goal of this work is to study reversible dissolution behavior of nanocrystals, i.e. dissolution of nanocrystals as a result of a true reversal of the growth reaction given according to Rempel et al.[39] in simplified form for *n*-sized CdSe nanocrystals of concentration, C_n, as

$$C_n + C_1 \leftrightarrow C_{n+1} \quad (1)$$

where n is the number of bound CdSe building blocks and C_1 is the concentration of free monomeric CdSe building blocks in solution, which are formed from cadmium and selenium precursor species. The dissolution studies described in our work are conducted in reaction environments commonly employed for CdSe nanocrystal QD synthesis and, therefore, are in strong contrast to typical nanocrystal etching reactions to uniformly reduce their size or induce crystal-face selective detachment of surface atoms. In these methods, nanocrystals are treated with chemical etchants such as hydrofluoric acid for InP,[42] tetrafluoroborate for CdTe[43] or with high concentrations of amines in the presence of oxygen and water for CdSe nanocrystals[35−37] to induce irreversible dissolution. In contrast, in our reversible dissolution/growth behavior study, we immerse presynthesized and purified, surface-stabilized CdSe nanocrystal QDs in octadecene (ODE) solvent containing long alkyl-chain fatty acid or amine ligands at elevated temperatures and under inert-gas atmosphere. Our strategy is to use purified nanocrystal QDs in the absence of any free monomeric CdSe species, C_1, in solution. Lack of C_1 should therefore shift eq 1 to

(41) Yu, W. W.; Qu, L.; Guo, W.; Peng, X. *Chem. Mater.* **2003**, *15*, 2854–2860.
(42) Talapin, D. V.; Gaponik, N.; Borchert, H.; Rogach, A. L.; Haase, M.; Weller, H. *J. Phys. Chem. B* **2002**, *106*, 12659–12663.
(43) Liu, J.; Yang, X.; Wang, K.; Wang, D.; Zhang, P. *Chem. Commun.* **2009**, 6080–6082.

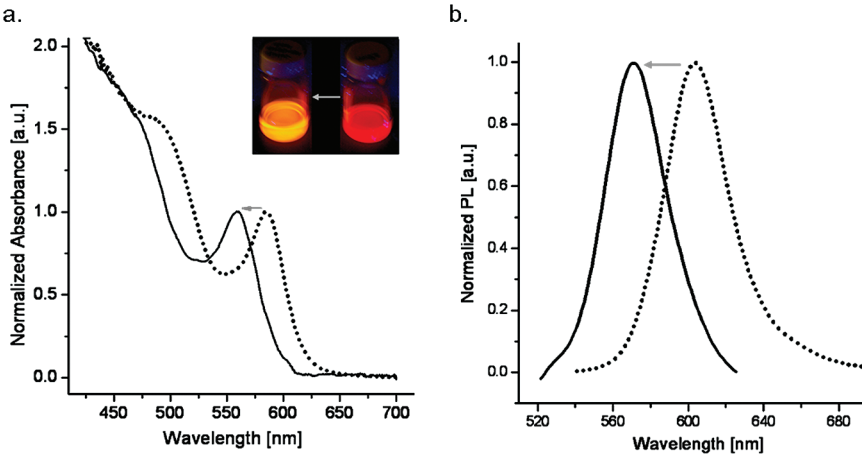

Figure 1. UV−vis absorption (a) and PL emission spectra (b) of CdSe nanocrystals before (···) and after (—) undergoing dissolution in the presence of ODA ligands. Inset: Corresponding PL emission image of the samples under UV lamp irradiation at 356 nm. All spectra were intensity-normalized for better comparison.

the left, resulting in nanocrystal dissolution. In the following we will describe the dependence of this dissolution process on various reaction parameters. The dissolution/growth behavior and accompanied change in size of the CdSe QDs were studied in situ by UV−vis absorption and PL emission spectroscopy and postreaction by direct TEM imaging of the nanocrystal QDs.

Figure 1 shows a typical dissolution behavior of CdSe nanocrystals. Figure 1a compares the UV−vis absorption spectra of a CdSe nanocrystal sample before (dashed gray line) and after (solid black line) a typical dissolution process. In detail, 1×10^{-6} mmol of purified CdSe nanocrystal QDs with an initial size of 4.0 nm were reacted for 60 min at 100 °C in 20 mL ODE containing 0.5 g ODA ligands. While both spectra have nearly identically shaped absorption features, the wavelength position of the first excitonic transition peak maximum of the treated sample is blue-shifted by about 35 nm. Using the CdSe QD sizing curves determined by Peng and co-workers[41] a size reduction from the initial 4.0 to 3.1 nm was calculated. This size reduction is also evident from the drastically changed PL properties shown in the inset in Figure 1a, which changed from red to yellow. The corresponding PL emission spectra of the samples before (dashed gray line) and after (solid black line) undergoing dissolution are given in Figure 1b. Comparison of the emission peak wavelength position shows the same blue-shifting trend as observed in the absorption spectra. In addition, an increase in the emission brightness was observed in the sample which is to be expected since amine-binding to QDs are known to increase their quantum yield.[38,44−47] Furthermore, the emission bands retained their typical full-width-at-half-maximum (fwhm) values of around 30 nm, indicating that the initial narrow QD size distribution is not influenced during the dissolution process. Under prolonged dissolution (several hours) however, we did observe slight broadening of the emission band. This size defocusing is the result of different dissolution rates for differently sized nanocrystals, increasing the natural QD size distribution with ongoing dissolution.

Dissolution of larger CdSe nanocrystal QDs was also monitored by TEM imaging. Figure 2a and b compare images of the nanocrystals before and after the dissolution event, respectively. We observed a size reduction from initially 5.5 ± 0.5 nm to 3.5 ± 0.5 nm, thus confirming that the observed changes in the optical/spectroscopic properties of the CdSe QDs are the direct result of the quantum size effect due to size reduction and not due to irreversible oxidation or other surface phenomena. Furthermore, high-resolution TEM investigations of the crystal lattice (given as insets in Figure 2) show intactness of the crystal structure after the dissolution. The TEM investigations are complimented by powder XRD characterization of the CdSe nanocrystals. Figure 2c and d show diffraction patterns of the CdSe nanocrystal QDs before and after dissolution, respectively. Both diffraction patterns display Scherrer-broadened reflections typical for nanocrystalline wurtzite CdSe with the prominent, broad and asymmetric peak centered at around 25° 2-theta, consisting of overlapped (100), (002), and (101) reflections and the two weak (102) and (103) reflections at 35.1° and 45.8° 2-theta.[48] The latter two reflections are strongly reduced in intensity for the QDs after the dissolution treatment. This observation together with the stronger Scherrer broadening is another consequence of nanocrystal size reduction, in accordance with results by Murray et al. who reported that as the nanocrystal size becomes smaller, lower intensity reflection peaks are more strongly affected than those of higher intensity.[13]

The temporal evolution of the absorption spectra under the dissolution conditions described above is presented in Figure 3a. It reveals that the dissolution is a continuous,

(44) Foos, E. E.; Wilkinson, J.; MÃkinen, A. J.; Watkins, N. J.; Kafafi, Z. H.; Long, J. P. *Chem. Mater.* **2006**, *18*, 2886–2894.
(45) Ji, X.; Copenhaver, D.; Sichmeller, C.; Peng, X. *J. Am. Chem. Soc.* **2008**, *130*, 5726–5735.
(46) Kalyuzhny, G.; Murray, R. W. *J. Phys. Chem. B* **2005**, *109*, 7012–7021.
(47) Nose, K.; Fujita, H.; Omata, T.; Otsuka-Yao-Matsuo, S.; Nakamura, H.; Maeda, H. *J. Lumin.* **2007**, *126*, 21–26.
(48) Talapin, D. V.; Nelson, J. H.; Shevchenko, E. V.; Aloni, S.; Sadtler, B.; Alivisatos, A. P. *Nano Lett.* **2007**, *7*, 2951–2959.

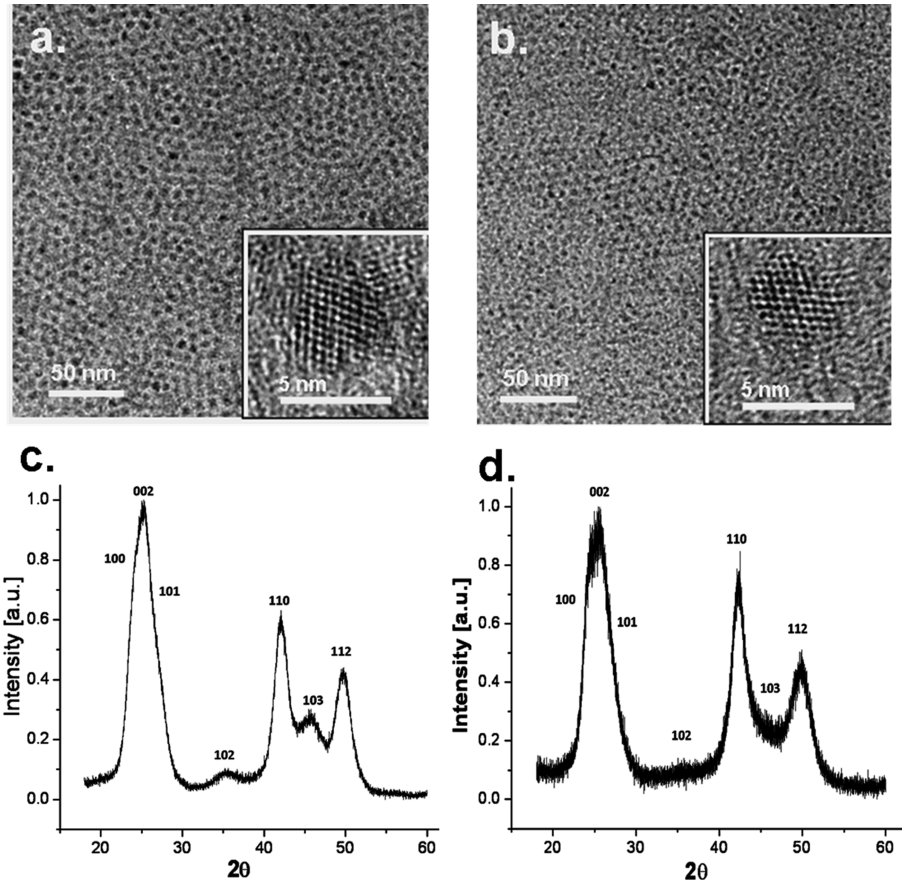

Figure 2. TEM images of colloidal CdSe nanocrystal QDs before (a) and after (b) undergoing dissolution in the presence of ODA ligands. Corresponding powder X-ray diffraction pattern of the samples before (c) and after (d) dissolution, intensity-normalized for better comparison.

gradual process of detachment of molecular building blocks rather than an uncontrollable, sudden fracture of nanocrystals into smaller units. In addition, we found the speed of this gradual detachment/dissolution process is highly dependent on the initial nanocrystal concentration. This is shown in Figure 3b, in which absorption (solid black lines) and PL emission (gray dashed lines) spectra of four samples with identical amounts of CdSe nanocrystal QDs and ODA ligands, but increasing amounts of ODE solvent are compared. All four samples were taken after keeping the samples at 100 °C for 60 min. Comparison of the spectra of the four treated samples to the spectrum of the same sample before treatment reveals significant blue-shifting of the first excitonic transition peak maximum in both the absorption and emission spectra for all four samples; however, the degree of blue-shifting (and thus nanocrystal dissolution) for a given reaction time increases with decreasing QD and free monomer concentrations (i.e., increasing dilution of the reaction mixture). This behavior is expected for a dissolution reaction as given in eq 1, since a lower free monomer concentration results initially in a stronger driving force for the reaction to shift to the left and, therefore, faster initial dissolution. To further study the role of free monomers to nanocrystal dissolution, we compared the rate of dissolution of purified versus "unpurified" samples of CdSe QDs. Here, "unpurified" refers to CdSe nanocrystal QDs for which the unreacted molecular cadmium and

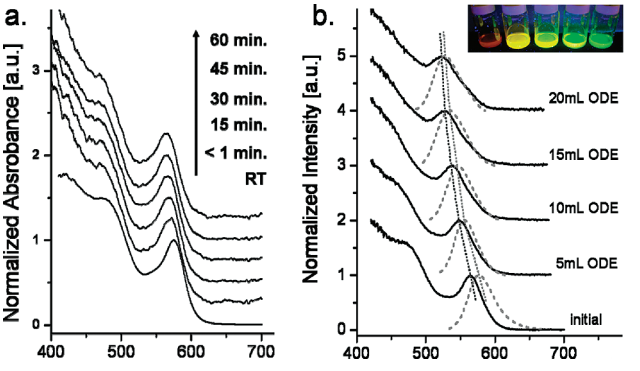

Figure 3. (a) Temporal evolution of the UV−vis absorption spectra of CdSe nanocrystal QDs during dissolution in the presence of ODA ligands at 100 °C for one hour. (b) UV−vis absorption (—) and PL emission (---) spectra of samples with decreasing CdSe QD concentration (increasing amount of solvent, ODE) dissolved in the presence of ODA ligands. All spectra were intensity-normalized for better comparison. Dotted lines are drawn to guide the eye.

selenium precursors have not been removed by repeated ethanol precipitation/hexanes dissolution. Under otherwise identical reaction conditions, the unpurified samples showed significantly lower dissolution rates (see Supporting Information Table S1), supporting the reversible dissolution-growth model as given in eq 1.

Effect of Ligands on Dissolution. The dissolution experiments described above were all conducted with additional amine ligands (ODA) present in solution. ODA was chosen since it is the most widely used ligand type for

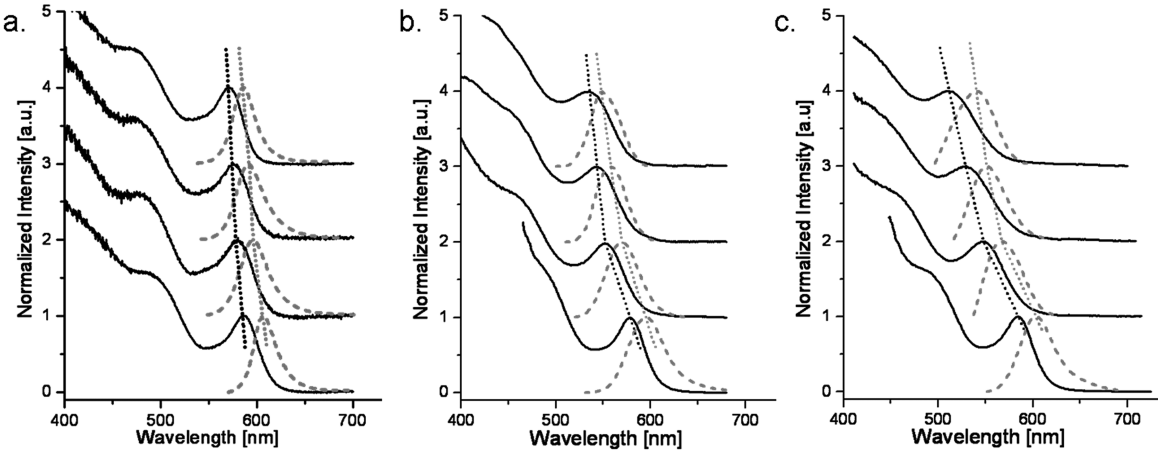

Figure 4. UV−vis absorption (—) and PL emission (---) spectra of samples with decreasing CdSe QD concentration (increasing amount of solvent, ODE; from bottom to top: sample before dissolution, 5 mL, 10 mL, 20 mL ODE) in pure ODE solvent (a), and in the presence of SA ligands (b), and OA ligands (c). All spectra were taken after dissolution at 100 °C for one hour. Spectra were intensity-normalized for better comparison. Dotted lines are drawn to guide the eye.

synthesis of high-quality colloidal CdSe nanocrystal QDs.[46,49−51] However, as mentioned earlier, amines are also known to act as nanocrystal etchants (especially in the presence of water and oxygen). To eliminate that the observed dissolution is a simple irreversible etching process, we repeated the dissolution studies in the presence of other ligand types and, most importantly, in the absence of any excess ligands. The results are given in Figure 4a (no added new ligands), Figure 4b (with SA), and Figure 4c (with OA) which shows the absorption and PL emission spectra of CdSe QDs immersed in increasing amounts of pure ODE solvent and kept at 100 °C for 60 min. It is important to note that in different ligand types and especially even without addition of any ligands, dissolution of nanocrystals occurs with the same time- and concentration-dependence as observed in the presence of ODA, that is, dissolution increases with increasing time and decreasing concentration. However, we also observed that the rate of dissolution was slower for reaction systems without added ligands. This can be explained by reduced stabilization of the detached/free CdSe monomeric units, C_1, in solution in the absence of excess ligands. As is also known from growth studies, ligand-binding to monomeric units is essential to keep them stable in solution.[50,52]

To obtain a broad insight into the ligand effect on dissolution, we studied a range of different ligands, including long alkyl-chain carboxylic acids (SA and OA), amines (ODA and octylamine, OcA), and the phosphonic acid ligand TDPA (tetradecylphosphonic acid). In general, dissolution occurs for all ligand types and amounts, albeit at different speeds. In fact, the reaction with TDPA ligands was so fast that the nanocrystals dissolved completely (loss of any CdSe QD-related absorption features) after only a few minutes at 100 °C, preventing any further studies with this ligand system. For the remaining carboxylic acid and amine ligands, we found that dissolution rates rapidly increase with increasing ligand-to-QD molar ratio, go through a maximum and then slowly decrease again. Maximum rates were observed in the range of $1-3 \times 10^6$ ligand-to-QD molar ratio, with the amines on the lower end of the range. In order to compare the effect of different ligands on the QD dissolution rate, we therefore used the same sized CdSe QDs for all experiments and kept the ligand-to-QD molar ratio constant at 5×10^5, well below the range of maximum dissolution rates. Here, the general trend for dissolution rates was found to be TDPA ≫ OA > SA > ODA > OcA > no ligands (see Supporting Information Figure S1). While the observed trend of phosphonic acids having larger dissolution rates than carboxylic acids is opposite to CdSe QD growth rates, it follows the ligand binding strength to the CdSe nanocrystal surface as phosphonic acids are reported to have the strongest binding affinity to CdSe out of this group of ligands.[52] The comparison between carboxylic acid ligands, which are potential metal-site-coordinating ligands via their oxygens[53,54] and amine ligands known to bind either by cadmium−nitrogen interactions or hydrogen bonding to selenium sites[55,56] is less conclusive as reported binding affinities strongly depend on the crystal faces of the CdSe lattice.[52,54] Nevertheless, the distinct difference in dissolution rates observed between these two ligand systems indicates strong overall differences in binding of these two type of ligands to the nanocrystal surface and to free monomers in solution.

Quantitative CdSe QD dissolution results for solutions without added ligands and those with OA, SA and ODA

(49) Li, J. J.; Wang, Y. A.; Guo, W. Z.; Keay, J. C.; Mishima, T. D.; Johnson, M. B.; Peng, X. G. *J. Am. Chem. Soc.* **2003**, *125*, 12567–12575.
(50) Pradhan, N.; Reifsnyder, D.; Xie, R.; Aldana, J.; Peng, X. *J. Am. Chem. Soc.* **2007**, *129*, 9500–9509.
(51) Bullen, C.; Mulvaney, P. *Langmuir* **2006**, *22*, 3007–3013.
(52) Puzder, A.; Williamson, A. J.; Zaitseva, N.; Galli, G.; Manna, L.; Alivisatos, A. P. *Nano Lett.* **2004**, *4*, 2361–2365.
(53) Rempel, J. Y.; Trout, B. L.; Bawendi, M. G.; Jensen, K. F. *J. Phys. Chem. B* **2005**, *109*, 19320–19328.
(54) Rempel, J. Y.; Trout, B. L.; Bawendi, M. G.; Jensen, K. F. *J. Phys. Chem. B* **2006**, *110*, 18007–18016.
(55) Al-Salim, N.; Young, A. G.; Tilley, R. D.; McQuillan, A. J.; Xia, J. *Chem. Mater.* **2007**, *19*, 5185–5193.
(56) Schapotschnikow, P.; Hommersom, B.; Vlugt, T. J. H. *J. Phys. Chem. C* **2009**, *113*, 12690–12698.

Table 1. Effect of Different Ligands on CdSe Nanocrystal QD Dissolution after 60 Minutes at 100 °C.[a]

vol. ODE [mL]	λ_{abs} [nm]	D [nm]	$\%\Delta V_{QD}$
initial	576	3.7	
sample with no ligand			
5	566	3.4	21
10	559	3.2	33
20	555	3.1	38
sample with SA			
5	553	3.1	41
10	550	3.0	44
20	539	2.8	55
sample with ODA			
5	562	3.3	28
10	558	3.2	34
20	542	2.9	52
sample with OA			
5	542	2.9	52
10	536	2.8	57
20	522	2.6	66

[a] QD sizes were determined according to the method described in ref 41 and uncertainties in the QD size evolution were calculated as 0.05-0.1 nm (see the Experimental Section for details). λ_{abs}, wavelength position of the first excitonic absorption peak; D, diameter of CdSe QDs; $\%\Delta V$, calculated QD volume loss in percent.

ligands are given in Table 1. Here, the wavelength position of the first excitonic absorption peak (λ_{abs}) and corresponding size (diameter, D) of CdSe QDs after 60 min of dissolution at 100 °C are compared. The last column lists the calculated volume loss of the CdSe QDs (under the assumption of spherically shaped particles), revealing the remarkable impact of dissolution. Even in the absence of any additional ligands the nanocrystals lost around one-third of their original volume due to dissolution within one hour, meaning that more than 30% of the originally bound CdSe units have detached from the QDs and are free in solution. In the presence of excess ligands the increased speed of dissolution results in the loss of up to two-thirds of the originally bound CdSe units. Moreover, we found that dissolution at 100 °C continued after one hour (although at slowed rates), confirming that dissolution dominates at this temperature.

The observed difference in dissolution rates for ligands with different binding affinities suggests that a dynamic ligand exchange at the nanocrystal surface takes place during the dissolution process. To test this we used solid state MAS NMR spectroscopy to compare the ligands present at the surface of CdSe QDs prepared in a ligand mixture of SA, TOP and TOPO before and after the dissolution process with excess ODA ligands (see also Supporting Information, Figure S2 and S3). As expected, $^{13}C-^{1}H$ and $^{31}P-^{1}H$ cross-polarization measurements revealed that the as-synthesized CdSe QDs have all three ligands used in the synthesis at their surface. After the dissolution (and purification) process, however, only the new ligand ODA was detected in significant amounts at the nanocrystal surface, confirming the dynamic ligand exchange during the dissolution process. In addition, to verify that the dissolution behavior is general and not

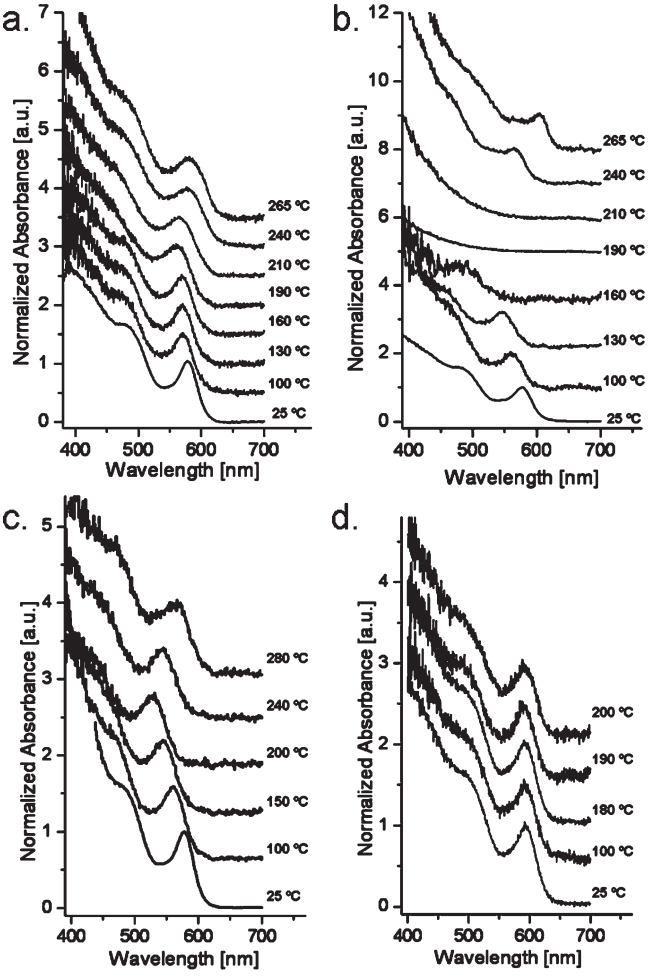

Figure 5. UV−vis absorption spectra of CdSe QDs in the presence of ODA (a) and SA (b−d) heated at different temperature intervals (as indicated in figures) to above the critical temperature. Heating rates between temperature steps were 1 °C/minute (a and b), 2−3 °C/minute (c and d). Note, sample shown in (d) was heated directly to above the critical temperature. All spectra were intensity-normalized for better comparison.

dependent on the ligands initially present on the QD surface, we also investigated CdSe QD stabilized initially by ODA ligands instead of SA/TOP/TOPO. Such QDs were synthesized following a method by Peng et al.[49] and qualitatively gave the same results as described above in terms of dependence of dissolution speed on ligand type, reactant concentration, and time (see Supporting Information Table S2). Comparing the degree of dissolution of similar sized CdSe nanocrystals treated in the same conditions, the SA/TOP/TOPO-capped ones dissolved more than the amine-capped ones.

Effect of Temperature on Dissolution. So far we studied CdSe QDs dissolution at low temperatures—far below their typical growth temperatures. In the following we will investigate the effect of temperature on the dissolution process. Figure 5a shows UV−vis absorption spectra of CdSe QDs (with an initial size of 3.7 nm) when heated in the presence of ODA. The sample was slowly heated (at about 1 °C/min) to the temperatures indicated in the figure. Once a given temperature had been reached a small amount of sample was withdrawn for optical

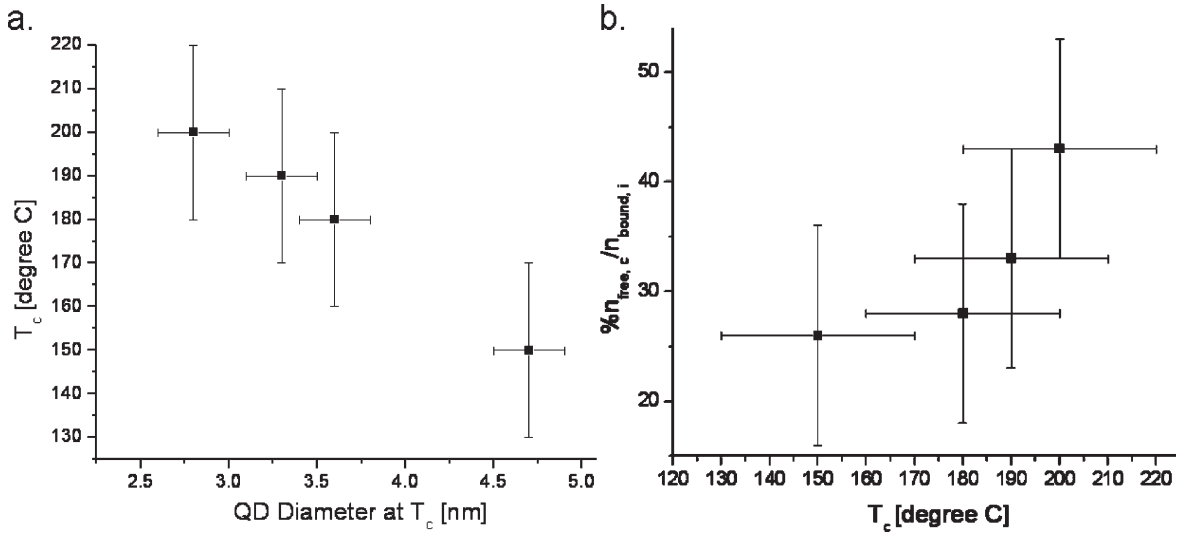

Figure 6. (a) Dependence of the critical temperature T_c on CdSe QD diameter for four samples with different initial sizes. (b) Fraction of CdSe monomeric species free in solution at T_c as a function of T_c for each of the four samples. The given T_c range is the result of experiments with CdSe nanocrystal QDs of the same size, but at different concentrations ranging from 2.2×10^{-7} M to 1.2×10^{-6} M). For all size ranges higher QD concentrations resulted in higher T_c values.

spectroscopy measurements and the sample was then heated to the next-higher temperature. Increasing the temperature from 100 to around 200 °C led to continuous QD dissolution indicated by increased blue-shifting of the first excitonic absorption peak. This blue-shift corresponds to the mean nanoparticle size reduction of 0.5 nm, which is equivalent to a loss of 33% of the original QD volume for this sample. However, upon further heating of the QDs beyond a critical temperature, T_c (in the range of 220−240 °C) red-shifting of the nanocrystal absorption features was observed, indicating the reversal of the dissolution process and regrowth of the nanocrystals—all the way to their original size.

Very similar temperature-dependent dissolution/growth reversibility is observed for CdSe QD samples heated in the presence of SA ligands. However, due to the higher dissolution speed of carboxylic acid ligands, using the same heating rates as with ODA can lead to the complete disappearance of any nanocrystal-related absorption feature, indicating the complete dissolution of the QDs (or at least dissolution to the point of extremely small crystallites that cannot be detected by our optical absorption measurements) as shown in Figure 5b. Nevertheless, the typical CdSe QD absorption feature reemerges upon increase of the temperature to above 220 °C and continuously red-shifts under prolonged treatment at these high temperatures. Interestingly, we observed that in cases in which the QDs were driven to dissolve far enough to lose any optical absorption signal, the red-shifting of the reemerged excitonic absorption peak often exceeds that of the original samples. For example, the sample shown in Figure 5b grew up to a final size of 4.8 nm whereas the size of the original sample was only 3.7 nm. Since no other molecular cadmium and selenium precursors other than that dissolved from the original QDs are available for the regrowth process, this strongly suggests the complete dissolution of the original CdSe QDs followed by nucleation of a new set of QDs upon temperature increase. This is also in agreement with our findings that in cases where the regrown nanocrystals had a larger size than the original ones, their final concentration was lowered (see also Supporting Information). In addition, it is worth noting that the dissolution/growth reversibility can be cycled multiple times. Finally, it should be emphasized that the degree of dissolution is simply dependent on the time the samples spends at temperatures below the regrowth temperature T_c. For example, Figures 5c demonstrates that under faster heating (around 2−3 °C/min) to temperatures above T_c (but otherwise identical reaction conditions) the same sample as shown in Figure 5b dissolves only partially before regrowth occurs. Moreover, when CdSe QDs are heated at even higher rates directly above T_c, their degree of dissolution is negligible. This is shown in Figure 5d and most likely also explains why dissolution is rarely observed under typically applied fast heating of CdSe nanocrystals in SILAR-type methods for coating them with layers of CdS or ZnS (core−shell structures) or for synthesizing other multilayer/multicomponent structures.[49]

We found that the dissolution-growth-reversal temperature (critical temperature, T_c) of CdSe QDs depends strongly on the QD size. This is shown in Figure 6a, which compares the critical temperatures for four differently sized QD samples. For each sample of a given size, three dissolution experiments with varying QD concentrations were performed. In detail, for each size 1.1×10^{-9} mol, 4.2×10^{-9} mol and 6.0×10^{-9} mol of CdSe QDs were dissolved in 5 mL ODE containing 0.5 g ODA ligands. To accurately track the critical temperatures for these samples, they were heated in only 10 °C increments and at each step sample aliquots were taken for spectroscopy. As given in Figure 6a, we observed that within a given QD size range the measured T_c values (defined as temperature at which blue-shifting of the excitonic absorption peak

Table 2. Amount of Bound and Free CdSe units per QD at the Critical Temperature T_c[a]

sample	T_c [°c]	D_i [nm]	D_c [nm]	$n_{bound,\ i}$ per NC	$n_{bound,\ c}$ per NC	$n_{free,\ c}$ per NC	$\%[n_{free,\ c}/n_{bound,\ i}]$
A	150	5.2	4.7	1292	959	334	26
B	180	4.0	3.6	596	429	168	28
C	190	3.7	3.3	485	325	160	33
D	200	3.4	2.8	372	211	161	43

[a] QD sizes were determined according to the method described in ref 41 and uncertainties in the QD size evolution were calculated as 0.05-0.1 nm (see Experimental Section for details). T_c, critical temperature; D_i, initial QD diameter; D_c, QD diameter at T_c; $n_{bound,i}$, number of initially-bound CdSe units per QD; $n_{bound,c}$, number of bound CdSe units per QD at T_c; $n_{free,c}$; number of free (detached) CdSe units per QD at T_c; $\%[n_{free,c}/n_{bound,i}]$, fraction of free (detached) CdSe units per QD at T_c.

wavelength position reversed to red-shifting) increased with increasing QD concentration. Between sets of differently sized QDs (with diameters between 5.2 and 3.4 nm) the critical temperature displayed an inverse proportional dependence on QD size. The finding that smaller QDs are less stable and require higher temperatures for switching from dissolution to regrowth can be explained by the increasing surface atom ratio with decreasing QD size. The surface atom ratio is the number of atoms at the surface of a given-sized QD divided by the total number of atoms and thus has a $1/r$ dependency.[15] The higher the surface atom ratio, the higher is the number of dangling bonds per nanocrystal. Smaller QDs therefore have a higher chemical potential and increased incentive to dissolve compared to larger ones.

The observation of QD-size-dependent dissolution-growth-reversal temperatures is of great importance since they mark states of equilibrium between dissolution and growth of CdSe QDs. Below this temperature, dissolution of QDs dominates (at varying rates depending on QD and monomer concentration as well as type and concentration of ligands in solution), whereas above T_c the trend is reversed and QDs regrow. The fact that even slightly below the dissolution-growth-reversal temperature QDs have the tendency to completely dissolve, while just slightly above it reattachment of the free (previously detached) monomers occurs, is an example of the mesostability of QDs. As pointed out by Peng and Peng, nanocrystals are thermodynamically mesostable systems for which it is impossible to reach an ultimate chemical equilibrium between nanometer-sized crystals and free monomers in solution—solubility thus becomes a relative term.[57] Nevertheless, as mentioned earlier, the chemical potential and thus the solubility of QDs is strongly dependent on their size (the smaller the size the higher their solubility). We studied this dependence by comparing the solubility of differently sized CdSe QDs at their respective critical temperatures—the equilibrium points of dissolution and growth at which the chemical potential of nanocrystals is equal to that of the free monomer units in solution. In the following, solubility is expressed as the degree of dissolution (i.e., the fraction of initially bound CdSe units per QD that detached during the dissolution process). This allows to easily account for different initial QD sizes and therefore different total numbers of bound CdSe units; in addition, as we will discuss later, this definition of solubility enables us to directly compare our results to those from growth studies.

The degree of dissolution at T_c of a given-sized QD sample was determined by first determining the QD size, D_c (the diameter at T_c) using UV−vis absorption spectroscopy. Under the assumption that CdSe QDs have a spherical shape, the number of bound CdSe units (n_{bound}) per QD can then be calculated according to eq 2

$$n_{bound} = \frac{D^3\pi}{6v_m} \quad (2)$$

in which D is the QD diameter and v_m is the CdSe molar volume.[58] Subtracting the number of bound CdSe units at T_c ($n_{bound,c}$) from the number of initially bound CdSe units ($n_{bound,i}$) results then in the number of free (detached) CdSe units ($n_{free,c}$). Finally, the fraction $n_{free,c}/n_{bound,i}$ gives the degree of QD dissolution at T_c. Results of this analysis are given in Table 2 for the four differently sized samples dissolved in the presence of ODA discussed above (see also Figure 6b) and clearly reveal the predicted size-dependence of QD solubility. While the largest QDs (D_c = 4.7 nm, T_c = 150 °C) display the smallest degree of dissolution with about 20% of the initially bound CdSe units in solution, this number steadily increases with decreasing QD size and reaches more than 40% for the smallest QDs tested (D_c = 2.8 nm, T_c = 200 °C). These findings not only confirm that the solubility of CdSe QDs is strongly size-dependent but also reveal that at the dissolution-growth equilibrium of QDs, a substantial amount of monomeric units are free in solution. We thus conclude that the condition of highest stability of colloidal CdSe QDs of a given size in solution is a state of equilibrium between the QDs and free monomer species of at least about 20% in solution. It should be emphasized that these results are in excellent agreement with aforementioned findings from growth studies of QDs by Alivisatos and co-workers, who also found an equilibrium state between QDs and free precursors in solution.[21] In detail, they reported that CdSe nanocrystals ceased to grow when there was still about 20−30% of molecular precursor in solution. Despite approaching the problem from opposite sides (growing vs dissolving QDs), both studies come to the same conclusion of a coexistence between the formed nanocrystal QDs and free

(57) Peng, Z. A.; Peng, X. *J. Am. Chem. Soc.* **2002**, *124*, 3343–3353.

(58) Jasieniak, J.; Mulvaney, P. *J. Am. Chem. Soc.* **2007**, *129*, 2841–2848.

molecular precursor species in solution being the most stable state.

Conclusions

The work presented here provides experimental evidence of the reversible dissolution-growth reaction of colloidal CdSe nanocrystal QDs with the driving force being the amount of free monomeric CdSe species in the reaction mixture. We conducted a systematic study of the dissolution behavior of purified CdSe QDs in solution. Experiments were designed to obtain a detailed insight into the relationship between growth and dissolution of QDs in solution as a function of QD size and concentration, the type and amount of ligands present in the solution, and the reaction temperature. Our model system consists of purified, surface ligand-stabililized colloidal CdSe nanocrystal QDs in a noncoordinating solvent under inert-gas atmosphere and at temperatures between 100 and 200 °C. We found that under these conditions, purified CdSe QDs undergo dissolution even in the absence of excess ligands in solution—with the rate of dissolution being inversely proportional to the QD concentration. In the presence of additional ligands, dissolution of QDs is faster than in pure solvent with rates depending on the binding affinity of the added ligands to the QDs.

Importantly, the dissolution process observed in this study is reversible and regrowth of QDs occurs by raising the temperature above a certain threshold. This threshold temperature at which QD dissolution reverses to growth is inversely proportional to the QD size. Moreover, the fraction of free (dissolved) CdSe monomeric units at the dissolution-growth-reversal temperature displays a typical QD solubility behavior with higher solubilities at higher temperatures. These findings show that the most stable state of colloidal CdSe nanocrystal QDs in solution is an equilibrium between formed nanocrystals and free monomeric precursors—a result also found in independent QD growth studies. In conclusion, we provide new insights into the stability of colloidal QDs in solution. In fact, preliminary studies show that this dissolution phenomenon is not restricted to CdSe nanocrystal QDs. We observed similar dissolution behavior also for lead chalcogenide nanocrystals and for core−shell type systems such as CdSe/CdS and CdSe/ZnS QDs. Our findings on QD dissolution thus should be of importance both for their long-term safe use in solution-based applications and, being the "back-reaction" of growth, for the rational design of synthesis routes for high-quality nanocrystals.

Acknowledgment. We thank Jeffrey Farrer (BYU Microscopy Lab) for help with TEM studies, Joel Miller for assistance with XRD measurements, and David Grant, Charles Mayne, and Mark Strohmeier for NMR studies. We are grateful to Eric Brauser and Lindsay Leone for valuable contributions. This work was supported in part by the National Science Foundation under Award No. ECS 0609244, a Utah Technology Commercialization Project grant, and by start-up funds from the University of Utah.

Supporting Information Available: Optical absorption and PL emission spectra of dissolution experiments of unpurified vs purified QD samples, using different ligands, and with differently synthesized nanocrystal QDs. Solid state NMR analysis data. Concentration analysis of QDs before and after a dissolution/regrowth cycle. This material is available free of charge via the Internet at http://pubs.acs.org.